ACS APPLIED MATERIALS & INTERFACES

www.acsami.org

Research Article

Graphene Oxide-Based Membrane as a Protective Barrier against Toxic Vapors and Gases

Cheng Peng, Zafar Iqbal, Kamalesh K. Sirkar,* and Gregory W. Peterson

Cite This: *ACS Appl. Mater. Interfaces* 2020, 12, 11094−11103

Read Online

ACCESS | Metrics & More | Article Recommendations | Supporting Information

ABSTRACT: Traditional protective garments loaded with activated carbons to remove toxic gases are very bulky. Novel graphene oxide (GO) flake-based composite lamellar membrane structure is being developed as a potential component of a garment for protection against chemical warfare agents (CWAs) represented here by simulants, dimethyl methyl phosphonate (DMMP) (a sarin-simulant), and 2-chloroethyl ethyl sulfide (CEES) (a simulant for sulfur mustard), yet allowing a high-moisture transmission rate. GO flakes of dimensions 300−800 nm, 0.7−1.2 nm thickness and dispersed in an aqueous suspension were formed into a membrane by vacuum filtration on a porous poly(ether sulfone) (PES) or poly(ether ether ketone) (PEEK) support membrane for noncovalent $\pi-\pi$ interactions with GO flakes. After physical compression of such a membrane, upright cup tests indicated that it can block toluene for 3−4 days and DMMP for 5 days while exhibiting excellent water vapor permeation. Further, they display very low permeances for small-molecule gases/vapors. The GO flakes underwent cross-linking later with ethylenediamine (EDA) introduced during the vacuum filtration followed by physical compression and heating. With a further spray coating of polyurethane (PU), these membranes could be bent without losing barrier properties vis-à-vis the CWA simulant DMMP for 5 days; a membrane not subjected to bending blocked DMMP for 15 days. For the PEEK-EDA-GO-PU-compressed membranes after bending, the separation factors of H_2O over other species for low gas flow rates in the dynamic moisture permeation cell (DMPC) are: α_{H_2O-He} is 42.3; $\alpha_{H_2O-N_2}$ is 110; and $\alpha_{H_2O-ethane}$ is 1800. At higher gas flow rates in the DMPC, the moisture transmission rate goes up considerably due to reduced boundary layer resistances and exceeds the threshold water vapor flux of 2000 g/(m^2·day) that defines a breathable fabric. This membrane displayed considerable resistance to permeation by CEES as well. The PES-EDA-GO-PU-compressed membrane shows good mechanical property under tensile strength tests.

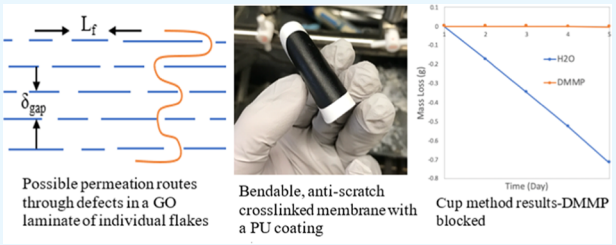

Possible permeation routes through defects in a GO laminate of individual flakes

Bendable, anti-scratch crosslinked membrane with a PU coating

Cup method results-DMMP blocked

KEYWORDS: *multilayer graphene oxide film, composite barrier membrane, chemical warfare agents, breathable fabric, diamine cross-linking, good mechanical properties*

1. INTRODUCTION

Novel materials and material structures have been investigated as a protective fabric/barrier for total protection from chemical and biological threat (CBT) including chemical warfare agents (CWAs).[1,2] The protective fabric should be breathable[3] and have excellent mechanical properties.

Traditional garments to protect against CBT use a high loading of sorbents, e.g., activated carbons, and are very bulky. Metal−organic frameworks (MOFs) having high surface areas and pore volumes are being explored for efficient CWA removal.[4] Such approaches target detoxification of the CWAs to prevent penetration for an extended time. Advanced highly ordered materials and nanomaterials that prevent penetration but are lightweight, flexible, and have high breathability are of particular interest. Graphene (GR)- and graphene oxide (GO)-based film structures are highly moisture permeable and almost impermeable to small gases;[5] these may block CWAs.

One-atom-thick, single-layer GR has a two-dimensional (2D) structure. The GR platelet aspect ratio is very high. Large amounts of GR in the form of GO can be made by Hummers' method.[6] However, reduced GO (rGO) so produced using different chemical agents yields only a GR-like structure but not the original GR. Spray coating of a dispersion of GO crystallites in water (produced by sonication[7,8]) on a Cu foil (with a small aperture) produced a 0.1−10 μm thick GO film, which had a high-moisture permeance, allowed traces of He in the presence of moisture but was almost impermeable to gases H_2, N_2, Ar, and ethanol.[5] Apparently, through GO nano-capillaries between closely spaced GR sheets, water monolayers flow but prevent other gases/vapors from flowing especially under reduced humidity. Separation studies using GO, rGO, and ultrathin GO membranes show: low gas permeability strongly affected by the presence of intercalated water;[9] isopropyl alcohol vapor permeability is strongly reduced in

Received: January 11, 2020
Accepted: February 3, 2020
Published: February 20, 2020

https://dx.doi.org/10.1021/acsami.0c00615
ACS Appl. Mater. Interfaces 2020, 12, 11094−11103

contact with water;[10] composite membranes of GO nanoplatelets show antibiofouling in wastewater treatment;[11] GO membranes on a ceramic hollow fiber exhibited selective water permeation over organics.[12]

To develop a CWA-rejecting membrane, recognize: a highly permeable poly(1-methylsilyl-1-propyne)-supported one-layer GR sheet via a chemical vapor deposition (CVD)-yielded a defective barrier.[13] Several-layered GR films had high O_2-N_2 selectivity; increasing layers decreased O_2 permeability. Defective GR sheets were irregularly aligned creating gas-permeable slit-like size-distributed interlayer spacing (as in carbon molecular sieve membranes, 0.355 nm average; graphitic layers, 0.335 nm).[13]

The GO membrane preparation method (vacuum filtration, direct evaporation, and spray and spin coating[13]) and interlayer spacing are important. The interlayer spacing of GO membranes can go up to 1 nm;[5] recent studies[14] show that it can attain 1.1−1.2 nm at 100% relative humidity (RH). A study[15] on water vapor transport through ultrathin GO membranes by grazing incidence X-ray scattering in air dehumidification experiments reveals interesting features: water vapor absorption follows a modified Kelvin equation revealing condensation in an elastic slit; GO interlayer distances vary between 7.2 and 11.5 Å depending on partial water pressures in the feed and the permeate; interstitial water quantity dictated by water partial pressure governs GO membrane performance.

The permeation of gases, e.g., CH_4, N_2, O_2, CO_2, and butane along with water vapor was studied[16] with RH variation through thin GO membranes supported on a porous Al_2O_3 membrane. Layered GO membranes at RH = 0 are essentially impermeable to small gases but allow H_2O vapor to go through. Under high humidity,[13] CO_2/N_2 selectivity of ∼20 was due to interaction with polar groups in GO. The transport of small gases, e.g., H_2, He, CO_2, N_2, O_2, depended on the degree of interlocking within the stacked GO structure. A heat treatment at 130−140 °C led to irreversible pore formation.

There is limited information on the transport of larger molecules, e.g., toxic gases/vapors and CWAs. The GR−elastomer bilayer structure consisting of a prestacked planar multilayer GO film on a prestretched elastomeric substrate was studied[17] for protection against organic solvents [e.g., hexane, chloroform, and trichloroethylene (TCE)] as well as for functioning as a sensor and subsequent actuation. GO membranes were studied as water-breathable barrier layers for the personal protective equipment[18] by measuring permeation of environmental toxicants, TCE and benzene. Another reference[19] demonstrated ultrabreathable and protective properties of membranes having sub-5 nm pores developed using carbon nanotube (CNT) pores; no toxic gas transport was studied.

A major transport pathway through ultrathin GO membranes was dimensionally selective structural defects in the GO flake instead of interflake spacing δ_{gap} (Figure 1).[20] High H_2 selectivity over CO_2 or N_2 was observed. H_2 and He permeances decreased exponentially with membrane thickness (1.8−180 nm) via high tortuosity (Figure 1). The structural defects rejected CO_2: selectivity $\alpha_{H_2-CO_2}$ was 250[20] at 100 °C; under pressure water permeance decreased drastically for rGO membranes.[5]

Multiple GO layers mask the effect of inevitable structural defects in GO flakes. The three dimensionality introduced by

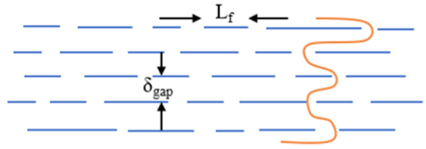

Figure 1. Possible permeation routes through defects in a GO laminate of individual flakes.

OH, COOH, and epoxy groups on a flake increases δ_{gap} to 1.2 nm.[14] Raman spectroscopy[21] and atomic force microscopy[22] were used to estimate the GR layer thickness, the membrane thickness, and the number of layers. Thermally reduced GO was studied[23] by imaging ellipsometry. The X-ray diffraction (XRD) technique of Liu et al.[14] is preferred for estimating the interlayer gap.

Functional group density in a GO flake is limited except at the highest oxidation levels and is likely to be present at the edges. The valence shell of sp^2-hybridized carbon atoms in a GR sheet possesses three σ electrons and one π electron. In a GO flake, the density of the π electrons will be high. Sulfonated poly(ether ether ketone) (PEEK) macromolecules are noncovalently adsorbed on the GR surface via $\pi-\pi$ interactions.[24] Any GO flake on a porous polymer surface will stick if there is a $\pi-\pi$ interaction; the substrate polymer should preferably have π electrons. We selected porous substrates of poly(ether sulfone) (PES) and PEEK to build a lamellar structure of GO flakes. We made barrier membranes of GO flakes blocking CWA simulants, e.g., dimethyl methyl phosphonate (DMMP) (a sarin-simulant for calibration of organophosphorus detectors), 2-chloroethyl ethyl sulfide (CEES) (the simulant for sulfur mustard) yet allowing high-moisture vapor transport. There is no such study. We characterized their permeation properties for a few gases and toluene vapor. Such barriers should be breathable, flexible, bondable to a porous substrate membrane, and be usable in a fabric.

2. METHODS AND MATERIALS

2.1. Chemicals and Gases. Single-layer graphene oxide (GO) flakes made by the modified Hummers' method were from Cheap Tubes (Grafton, VT). The GO dimensions were 300−800 nm with a thickness of 0.7−1.2 nm. GO flakes were also obtained from Angstron Materials (Dayton, OH): the GO flake dimensions were ∼7 μm with 2−3 nm thickness. Sodium dodecyl sulfate (SDS) (ACS reagent, ≥99.0%), ethylenediamine (EDA) [puriss. p.a., absolute, ≥99.5% (GC)], and DMMP (97%) were bought from Sigma-Aldrich. Polyurethane (PU) spray was from Minwax (Minwax fast-drying semigloss oil-based polyurethane: Minwax, Upper Saddle River, NJ). Methanol (GR ACS) was bought from EMD Millipore (Billerica, MA). Gas cylinders of He, N_2, and ethane were from Airgas (Piscataway, NJ). CEES was obtained from Millipore Sigma (97%).

2.2. Support Membranes and GO. The poly(ether sulfone) membrane (Sterlitech, Kent, WA) was earlier selected as the substrate because of its benzene rings, which can develop noncovalent $\pi-\pi$ interactions with graphene. Later studies explored a flat microporous PEEK membrane (200 nm pore size)[24] (Sterlitech) as the support. It has high organic resistance; PES has much less. Membrane parameters are shown in Table S1.

2.3. Preparation of GO Flake Suspension. Initially, 4 mg of the GO powder was added to 40 mL of deionized (DI) water (the use of 20 mL was also explored); 16 mg of SDS (4 mg SDS/mg of GO) was added as a dispersant. Different GO amounts, 1, 2, and 3 mg, were used for specific experiments. Later, it was found that 3 mg of SDS/mg of GO was enough for a good dispersion. The ultrasonication was employed until a clear dispersion was obtained. The ultrasonication

https://dx.doi.org/10.1021/acsami.0c00615
ACS Appl. Mater. Interfaces 2020, 12, 11094−11103

time was increased from 15 to 60 min to get a more uniform dispersion. However, this led to a dispersion, which became too warm, which could affect the substrate structure. Therefore, the time was reduced to 45 min; the suspension was allowed to cool down to room temperature for 5 min. For our studies reported here, 45 min ultrasonication time was used.

2.4. Un-cross-Linked GO Membrane Preparation on the PES Support Membrane. The PES membrane was placed on a vacuum filter holder (Fritted Support Assembly, 47 mm, VWR, PA). The suction filtration was carried out to remove water and SDS completely (wash several times with DI water until no foam was observed in the exhaust pipe). A long neck dropper was used to add water slowly and carefully to avoid flushing the GO layers away when washing it to remove the SDS. The membrane surface appeared to be smoother. This will indicate that the membrane structure is more uniform suggesting that the GO layers are likely to be stacked in a more orderly fashion (Figure 1) to reduce the number of large defects. It was more difficult to prepare a clear dispersion with GO from Angstron Materials compared to that with GO of smaller dimensions from Cheap Tubes; much more SDS had to be added. After filtration, the membrane was taken out and slowly dried in an oven in N_2 at 40 °C.

2.5. Cross-Linked GO Membrane Preparation on the PEEK/PES Support Membrane. While retaining the permeation properties of the GO membrane, the membrane still needs to be mechanically stronger and more ductile for purposes like making clothes. EDA was selected as the cross-linking agent with GO.[25] The corresponding membrane making process was as follows.

The GO powder (8 mg) was added to 100 mL of deionized water; 16 mg of SDS was added as the dispersant. The ultrasonication was used until a clear dispersion was obtained. Then, 6 g of EDA was added to 40 mL of cold deionized water, and then more cold water was added to lower the temperature of the solution. The reason for keeping the solution cold was to prevent an observed increase in viscosity due to the potential lowering of critical micelle concentration of SDS and the corresponding micellization in the presence of amines. The diamine solution was slowly mixed with GO dispersion with stirring.

Then, the substrate hydrophobic PEEK membrane was placed on the vacuum filter holder and was fixed. Several drops of methanol were added to the hydrophobic PEEK membrane to wet it. Next, suction filtration was carried out to remove all the water and SDS (wash several times with EDA solution with the same concentration in case EDA might be washed away during this process, until no foam can be observed in the pipe); this usually took 2−3 days.

The membrane was then taken out and slowly dried in an oven in a N_2 atmosphere at 40 °C. The membrane was subjected next to physical compression (see Section 2.6). Then, the membrane was put back into the oven at 80 °C for an hour to create cross-linking with the amine between various functional groups sticking out of the edges of GO flakes. In the end, a polyurethane coating (~2 μm thick) on top of the GO membrane was developed via spray coating. An hour gap was provided after coating each time with a total of three coats. Next, the membrane was dried slowly for 48 h before testing. Such membranes were designated PEEK-EDA-GO-PU. The PU-coated side faces the feed gas/vapor during experimental permeation studies.

This method was also carried out with the PES substrate membrane instead of the PEEK substrate membrane. The only difference with the above-mentioned procedure was that the step involving the wetting of the membrane with methanol was not needed with the PES substrate. Such a membrane was designated as PES-EDA-GO-PU. A graphical illustration of the fabrication procedure ending with a polyurethane coating is provided in Figure S1 (Supporting Information, SI).

2.6. Compression of GO Membranes. In the GO membranes prepared, GR flakes are not all stacked horizontally. Instead, they stack at an angle increasing the gap between GO layers and let more gases/vapors go through. The GO membranes prepared were therefore often subjected to physical pressure-based compression using a tableting machine (model 3853-0, CARVER, Inc., Wabash, IN) for 2 min. This compression was done with the membranes in steps for membrane making described under Sections 2.4 and 2.5.

2.7. Thickness Measurement and Fourier transform infrared (FTIR) Characterization. Research was conducted on measuring both the thickness of the GO membrane and the thickness of the interlayer. Scanning electron microscopy (SEM) [(1) JSM-7900F field emission SEM, JEOL USA, Inc.; (2) LEO 1530VP-Zyvex Nanomanipulator System/Cryo-system, Zeiss, Thornwood, NY] and transmission electron microscopy (TEM) (Hitachi H-7500) were used to determine the GO membrane thickness and its interlayer morphology. An Empyrean multipurpose diffractometer with a PIXcel1D detector (Serial 202627, PANalytical) was used to obtain the spectra of GO membranes on the PES support as well as the PEEK support membrane. XRD patterns of samples were scanned by Cu K(α) radiation (λ = 1.54 Å, 40 mA, 45 kV) from 5 to 60° of 2θ, step size = 0.0260° (2θ) to provide guidance on different values of the interlayer gaps. The samples for XRD were kept in closed sample containers but were exposed to the XRD equipment environment. For FTIR (Agilent Cary 670 FTIR Imaging Microscope, Agilent, Santa Clara, CA) spectra of samples, 32 scans were taken for each sample over a range of 6000 to 400 cm^{-1} with a resolution of 4 cm^{-1}.

2.8. Gas Permeation Setups and Permeability Measurements. The gas permeation apparatus using crossflow and based on the concept of the dynamic moisture permeation cell (DMPC)[26] is shown in Figure S2. A pressure gage was added to each of the feed side inlet and sweep side inlet to ensure that the pressure difference between the two streams was very low. Mass flow controllers were used at the feed inlet, the sweep inlet, and the sweep outlet. The membrane area in the cell was 7.07 × 10^{-4} m^2. More details are provided in Section S.1, SI.

Permeability measurement studies for dry N_2 permeation were made through a GO membrane using a thermal conductivity detector. In addition, a flame ionization detector (FID) was used also for permeation measurements of organic gases/vapors. Details for permeability measurement of He and water vapor at 25 °C are in Section S.1. The humidity of the feed gas was usually around 96%.

Permeation rate measurements carried out initially with un-cross-linked and cross-linked GO membranes utilized a low gas flow rate of 20 cm^3/min for both feed and sweep gas streams on two sides of the membrane. These experiments involved determination of permeabilities of N_2, He, and ethane along with that of moisture. When individual permeabilities of N_2 and ethane were determined with N_2 or ethane as the feed gas, the humidifier was detached from the setup. So, there was no moisture in the feed gas. He was used as the sweep gas. When moisture permeability was being determined, N_2 was humidified and passed on the feed side and He on the sweep side. No N_2 permeability measurement was made in such runs by the gas chromatograph (GC).

It is known that boundary layer resistances are quite important;[26] therefore, gas flow rates on both sides of the membrane were important. The effect of gas flow rate variation on individual gas permeation rate was also examined for the transport of moisture and N_2 at flow rates of 20, 50, 100, 200, and 500 cm^3/min (same value on both sides).

Equation S.1 in the SI defines gas/vapor permeance of species i: (Q_{im}/δ_m).[27,28] Using individual gas species permeances, one can define a separation factor between species i and species j

$$\alpha_{ij} = \frac{(Q_{im}/\delta_m)_i}{(Q_{jm}/\delta_m)_j} \quad (1)$$

Permeation studies were also made using the "upright cup method"[29,30] (Figure S3 and Section S.2), which employs diffusion without any bulk flow resulting in high boundary layer resistances.

The CEES permeation testing was conducted to determine barrier properties against a chemical warfare agent simulant. The testing was conducted per ASTM F 739-12. A swatch was cut and placed within a 1 in. diameter Pesce PTF 700 permeation cell. Dry air at 300 mL/min was applied countercurrently above and below the test swatch. CEES was fed from a saturator cell at a rate necessary to achieve 300 mg/m^3.

https://dx.doi.org/10.1021/acsami.0c00615
ACS Appl. Mater. Interfaces 2020, 12, 11094−11103

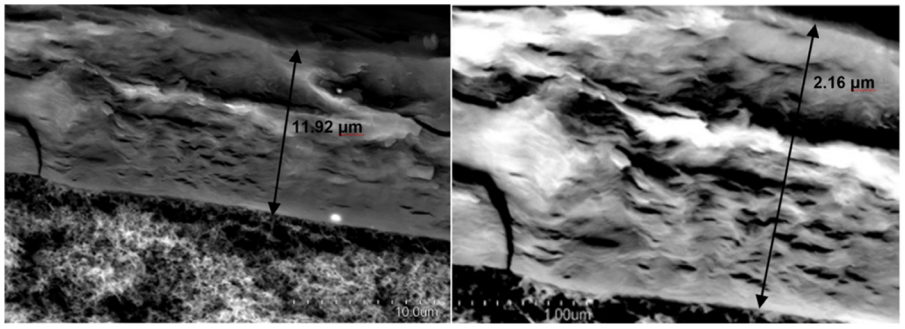

Figure 2. Left-hand side SEM micrograph shows the layer by layer structure of the 4 mg based GO membrane; the right-hand side SEM micrograph shows the cross-section of the 4 mg based GO membrane after compression.

The test was terminated when the steady state was reached and the permeate and retentate stream concentrations equaled the feed concentration accounting for the dilution in the permeate.

2.9. Tensile Strength Measurements of GO Membranes. Tensile strength tests were carried out using the Instron model 3342 Testing System (Instron, Norwood, MA). Samples were cut into 10 mm × 30 mm rectangular strips and were held in the testing machine sample holder. The load was slowly increased to get the tensile stress/strain plots. The slope of the stress−strain curve is Young's modulus.

3. RESULTS AND DISCUSSION

3.1. Un-cross-Linked GO Membranes on PES: Thickness Measurement and Compression. A number of membranes were made by vacuum filtration of a GO slurry on a porous PES support membrane. A series of GO membranes were prepared using the process Section 2.4, but with different amounts of GO in dispersion (with 1, 2, 3, and 4 mg of the GO powder) all other conditions remaining the same. A few such membranes are shown in Figure S4. As the GO concentration decreases, the color of the membrane became less dark.

The thicknesses of this series of GO membranes were measured by SEM; the micrographs are shown in Figure S5. Figure S5a−d corresponds to membranes made with 4, 3, 2, and 1 mg of GO. As the GO content decreases, the membrane thickness decreases (the color becoming lighter, Figure S4).

The left-hand side of Figure 2 shows the cross-section of a GO flake-based membrane structure for a 4 mg GO-based membrane obtained by SEM. From the calculations for the average gap between the consecutive GO laminate layers shown in Section S.3 (SI) along with Figure S6 for GR, it appears that the average gap between the consecutive GO layers is ≈2.21 nm for the 4 mg GO-based membranes. What happens to this value when the 4 mg GO-based membrane is compressed is shown in a SEM on the right-hand side of Figure 2. The irregular stacking and the gaps between layers were decreased; the thickness is reduced to 2.16 μm. For the 4 mg based GO membrane subjected to compression, the average gap distance between layers should then become 2.16 μm/5400 ≈ 0.4 nm since calculations in Section S.3 indicate 5400 layers in this membrane.

One can use XRD to explore the gap distance[14] between consecutive layers of GO in such membranes, which were not subjected to compression. Figure 3 provides the XRD patterns for both 2 and 4 mg GO-PES membranes showing a diffraction peak at 2θ = 18.20°, which corresponds to an interlayer spacing of about 0.49 nm. The 4 mg GO membrane has another peak, which appears at 2θ = 9.05°; the corresponding interlayer distance calculated for this 4 mg sample is 0.978 nm.

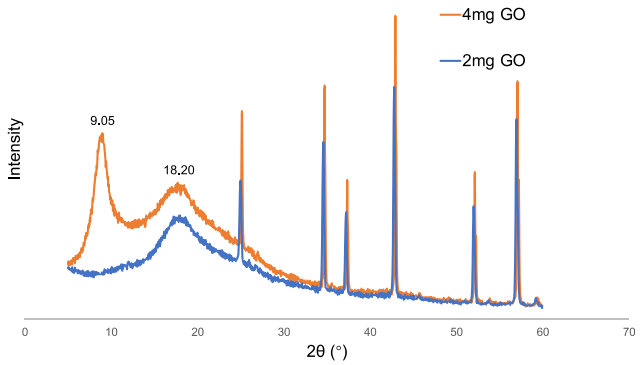

Figure 3. XRD scans of a 4 and a 2 mg GO-based membrane on a PES substrate; these membranes were not subjected to compression.

Different peaks in the interlayer spacing of this GO membrane result from the disorder that exists in the as-formed GO-PES membrane. The disorder increases as the membrane thickness increases. The 2 mg membrane hardly shows much XRD intensity for the larger gap of 0.978 nm due to a lower level of disorder. The sharp peaks located from 25 to 60° all belong to the PES substrate.

3.2. Gas Permeation Behavior of Un-cross-Linked GO Membranes. Gas/vapor permeation tests were run with the un-cross-linked GO membranes shown in Figures S4 and S5. The permeances of various gases and vapors obtained are shown in Table 1. Figure S7 graphically illustrates the relation between species permeance and the membrane thickness for He, N_2, an organic vapor (C_2H_6), and water vapor (data collected with the 20 cc/min gas flow rate on two sides of the membrane in the DMPC cell.) The effect of the feed and the sweep gas flow rate will be considered later. Note that there was no moisture in the system for N_2, ethane, and He.

Table 1. Species Permeances[a] with PES Substrates for Different Un-cross-Linked Membrane Thicknesses Due to Different GO Amounts for Several Gases/Vapors

		permeance [×10^9 mol/(s·m^2·Pa)]			
usage of GO (mg)	thickness (μm)	He	N_2	ethane	H_2O
4	11.92	5.0	3.1	1.4	226
3	8.01	7.1	3.3	1.7	152
2	1.46	20.0	5.1	2.8	149
1	0.84	46.1	18.5	15.9	128

[a]Data taken with the 20 cm^3/min gas flow rate on both sides of the membrane in DMPC.

https://dx.doi.org/10.1021/acsami.0c00615
ACS Appl. Mater. Interfaces 2020, 12, 11094−11103

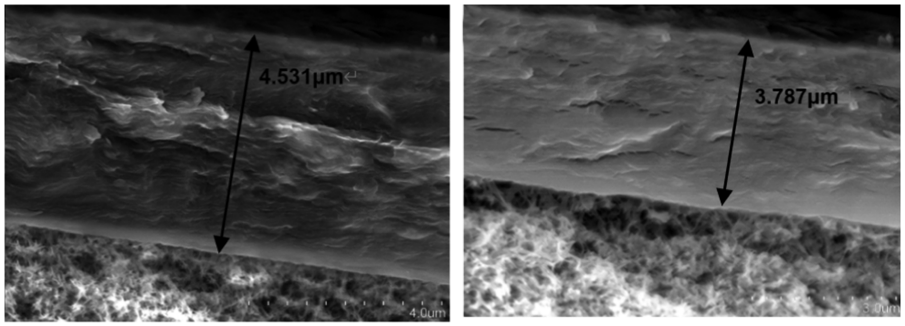

Figure 4. SEM micrograph of the cross-section of the compressed 8 mg GO membrane on PES support after washing for 1 week (left side) and 2 weeks (right side) (thickness: left: 4.53 μm; right: 3.78 μm).

It is clear from Table 1 and Figure S7 that gas permeance drops with the increasing membrane thickness for all species except water vapor. Also, the larger is the kinetic diameter of the gas/vapor, the lower is its membrane permeance with ethane possessing the largest kinetic diameter having the lowest permeance. Water vapor permeance has a unique behavior, as it does not show a clear relation with the membrane thickness except it appears to be significantly higher for the 4 mg membrane. We postulate that higher membrane thicknesses resulting from higher GO usage would lead to a higher level of disorder between the consecutive layers (as shown in Figure 3). Water monolayer transport[5] through GO nanocapillaries of larger dimensions between closely spaced GR sheets would therefore be enhanced. The permeation rates of the three gas species studied were quite low. Since there was no moisture during their permeability measurements, their permeances decreased as the layer numbers increased with an increase in the membrane thickness.

Remarkably, the permeance of water vapor is much higher. At the highest membrane thickness, the water vapor permeance is more than 150 times that of ethane. It is expected that when larger size organic vapors appear, extraordinarily high selectivity for water vapor will be achieved and probably the larger organic vapor species may be blocked. With the 4 mg GO membrane, the separation factors of H_2O over various other species calculated using mole-based permeances are as follows: α_{H_2O-He} is 45.2, $\alpha_{H_2O-N_2}$ is 72.9, and $\alpha_{H_2O-ethane}$ is 161.4.

After compression of the un-cross-linked GO membrane, the irregular stacking and the gaps between layers were decreased. The modified process described in Section 2.5 without cross-linking and PU coating was used here with 8 mg of GO powder with 80 mL of DI water and 24 mg of SDS to make the membrane. Those changes also led to a longer time of washing to remove the SDS (about 10 days). The presence of SDS in the interlayer region increases the interlayer gap leading to potentially reduced selectivity of water vapor vis-à-vis larger species. The SEM pictures of these membranes are shown in Figure 4.

The compression of the un-cross-linked GO membranes leads also to somewhat lower permeances of various gases/vapors, as shown in Table 2. For comparison, the data on 4 mg membranes without compression are shown also in Table 2 at the beginning.

Two separate tests were run using the upright cup method with water and toluene for 5 days using the 4 mg based membrane (see Figure 5a and Table S2). Note: for each pure liquid in the cell, it is a separate run even though we are showing the results for two liquids in the same Figure 5a and Table S2. It can be easily calculated that water vapor permeance is $\sim 1.3 \times 10^{-7}$ mol/(s·m^2·Pa) (similar to that in Table 2), while for toluene, the membrane is nearly impermeable. But the 4 mg GO membranes with compression did not totally block toluene. It appears that a significant mass loss with toluene starts showing up after 3 days. Figure 5b and Table S2 also show the corresponding data for 8 mg membranes. A significant mass loss with toluene starts appearing somewhat later after 4 days. Mass loss results shown in Figure 5c and Table S3 employed upright cup method tests for the 8 mg GO-based membranes prepared via Section 2.4 on the PES support membrane for DMMP and water in separate experiments as test liquids. It appears that the mass loss with DMMP is vanishingly small even after 5 days. A linear mass loss for water vapor can be observed in all plots in Figure 5.

Table 2. Gas/Vapor Permeances[a] of Compressed 4 and 8 mg Un-cross-Linked GO Membranes by DMPC

		permeance [$\times 10^9$ mol/(s·m^2·Pa)]			
usage of GO (mg)	thickness (μm)	He	N_2	ethane	H_2O
4 (without compression)	11.92	5.0	3.1	1.4	226
4	2.16	3.8	1.8	1.0	172
8 (1 week washing)	4.53	2.5	1.2	0.81	154

[a]Data taken with 20 cm^3/min gas flow rate on both sides of the membrane in DMPC.

The kinetic diameter for toluene is 0.65 nm and DMMP is 0.57 nm.[31] They are both larger than 0.4 nm, which is the estimated average gap distance between GO layers after compression (further details on the interlayer gap will be provided soon). The visible mass loss for toluene after 4−5 days resulted from poor chemical resistance of PES against aromatic hydrocarbons. Toluene swells PES, destroying its structure and causing leakage to occur earlier than that for DMMP. After taking the membrane out of the cell, we observed that the substrate membrane was essentially almost ruptured by swelling with toluene, which affected the stability of the GO layer on its top. This suggested the use of the PEEK substrate.

3.3. Cross-Linked GO Membrane. FTIR was used to identify the cross-linking in the GO membrane. As shown in Figure 6, the C−N stretching mode line around 1050 cm^{-1} is somewhat weak but shows the characteristic absorption lines of EDA−GO cross-linking. Other relevant peaks correspond to alkoxy (C−O) at 1029 cm^{-1}, carboxy (C−O) at 1377 cm^{-1},

https://dx.doi.org/10.1021/acsami.0c00615
ACS Appl. Mater. Interfaces 2020, 12, 11094−11103

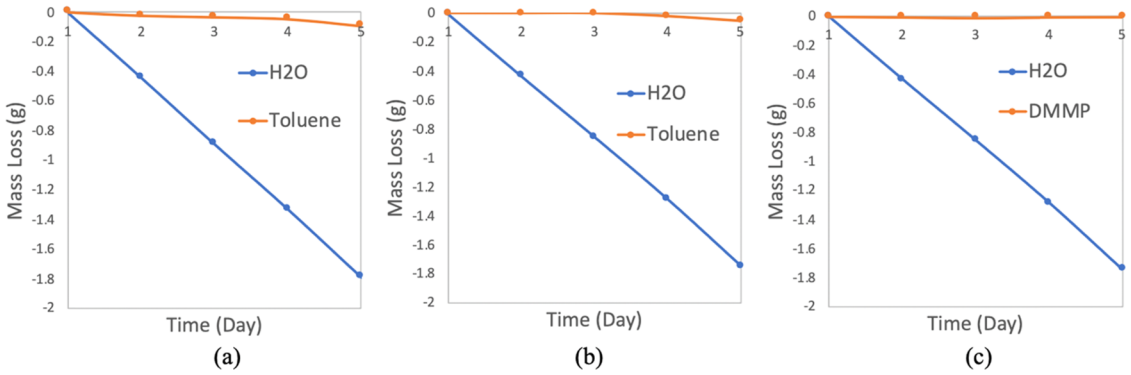

Figure 5. Upright cup method plots of mass loss vs time in days for separate experiments with water vapor and toluene/DMMP, respectively, using un-cross-linked GO membranes on a PES support membrane after compression: (a) water vapor and toluene, 4 mg GO membrane; (b) water vapor and toluene, 8 mg GO membrane; and (c) water vapor and DMMP, 8 mg GO membrane.

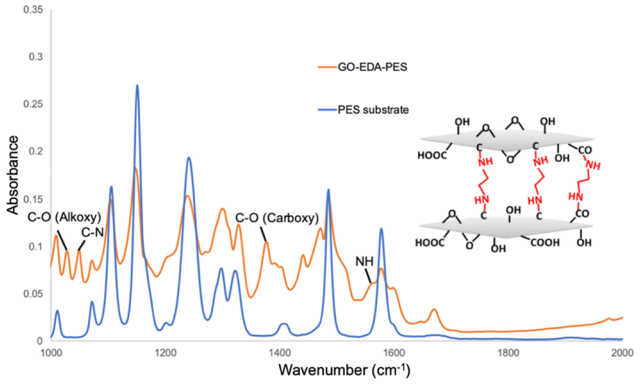

Figure 6. Ethylenediamine (EDA) cross-linked with GO flakes (shown as the inset on the right)[18,25] and FTIR spectra between 1000 and 2000 cm^{-1} of EDA−GO cross-linked on the GO membrane as described in Section 2.5 on a PES substrate membrane (larger, on the left in orange) along with that of the poly(ether sulfone) substrate (in blue).

and N−H at 1560 cm^{-1}. The peaks of the substrate membrane of PES are quite strong. A photo of the PEEK-supported cross-linked GO membrane developed using the process described in Section 2.5 is shown in Figure S8.

The mechanical property of this membrane was greatly improved by cross-linking. As shown in Figure 7, it can be rolled or bent multiple times without showing any cracks; this was not possible earlier. The polyurethane coating provides an antiscratching layer. Permeation tests were carried out using the upright cup method for a few membranes. Figure 8a,b shows, respectively, the upright cup method results for DMMP and toluene using cross-linked GO membranes (with PU coating) prepared on a PEEK membrane substrate. As before, these involve separate experiments with each liquid including water if shown. There was no leakage of either DMMP or toluene over the 5 day period.

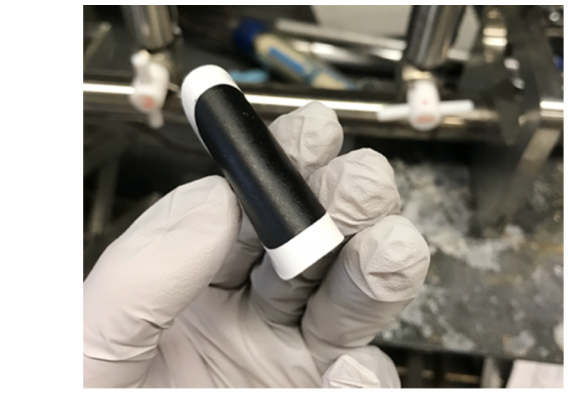

Figure 7. Demonstration showing that due to the use of a cross-linking agent, the membrane can be rolled or bent multiple times without developing any cracks.

Figure 8c illustrates the upright cup method results for DMMP carried out for 15 days with no weight loss at all. In a similar experiment with water, all water was gone by the 8th day.

The PEEK substrate has good chemical resistances against aromatic hydrocarbons; so, it was used to support the GO membrane to specifically deal with organic vapors such as toluene. Although it blocked toluene for 5 days, the polyurethane coating facing toluene vapor underwent large swelling and its shape appeared quite distorted after the test. With DMMP, we did not see any such effects. It is clear that these types of membranes have good mechanical and permeation properties. Table 3 provides permeation data by the upright cup method for cross-linked membranes before and after bending. For DMMP, there is hardly any difference. Therefore, the EDA cross-linked membranes have made good progress toward usability. Note: the GO membranes in ref 18 allowed a significant permeation flux of benzene but reduced the flux of trichloroethylene substantially.

Table 4 illustrates the permeance data for various gases/vapors using the DMPC method for PEEK-EDA-GO-PU membranes before and after bending. The data in Tables 3 and 4 show that this type of cross-linked GO membrane retains good performance even after bending multiple times. Based on Table 4 data for PEEK-EDA-GO-PU membranes after bending, the separation factors of H_2O over various other species are as follows: α_{H_2O-He} is 42.3, $\alpha_{H_2O-N_2}$ is 110 and $\alpha_{H_2O-ethane}$ is 1800. Note: water vapor permeance per this table is around 145 × 10^{-9} mol/(s·m^2·Pa) which is close to the upright cup method value 130 × 10^{-9} mol/(s·m^2·Pa) from the data in Figure 5a. It shows that the reduction in water vapor permeability due to GO cross-linking is not substantial. However, the permeances of other gases and vapors do get reduced significantly. Cross-linking leads to a membrane with good permeation performance for moisture in addition to excellent selectivity over small gases/vapors.

https://dx.doi.org/10.1021/acsami.0c00615
ACS Appl. Mater. Interfaces 2020, 12, 11094−11103

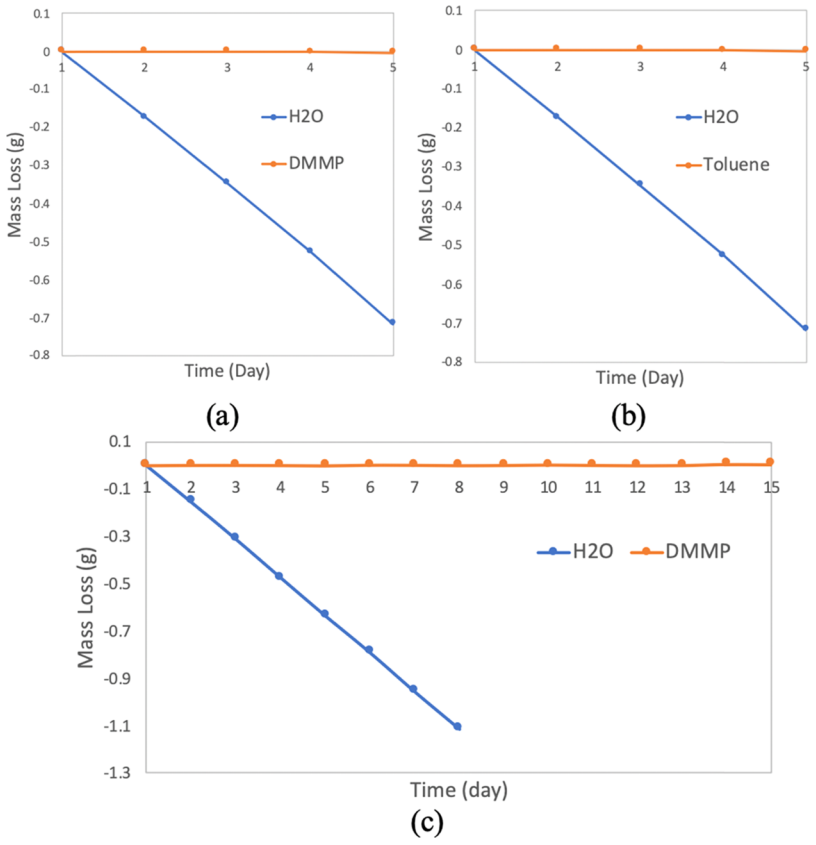

Figure 8. Upright cup method plots of mass loss vs time in days: (a) water vapor and DMMP for 5 days for PEEK-EDA-GO-PU; (b) water vapor and toluene for 5 days for PEEK-EDA-GO-PU; and (c) water vapor and DMMP for 15 days for PEEK-EDA-GO-PU.

Table 3. Upright Cup Method Results for Water[a] and DMMP for PEEK-EDA-GO-PU Membranes before and after Bending

days	1	2	3	4	5
mass loss GO/H_2O (g)	0	−0.1759	−0.3491	−0.5302	−0.7062
mass loss GO/DMMP (g) (before bending)	0	−0.0004	0.0002	0.0002	0.0005
mass loss GO/DMMP (g) (after bending)	0	0.0002	−0.0001	−0.0002	0.0001

[a]Separate experiments were done first with water and then with DMMP using the same membrane.

Table 4. Permeances[a] of PEEK-EDA-GO-PU Membranes for Various Species before and after Bending by DMPC

		permeance [$\times 10^9$ mol/(s·m^2·Pa)]			
usage of GO (mg)	thickness (μm)	He	N_2	ethane	H_2O
8 (before bending)	6.10	3.4	1.2	0.09	146
8 (after bending)	6.10	3.4	1.3	0.08	144

[a]Data taken with 20 cm^3/min gas flow rate on both sides of the membrane.

It is important to explore further as to what is the true moisture permeation rate of these membranes by reducing the boundary layer resistances. Experiments were carried out in the setup containing the DMPC with different flow rates of the feed gas and the sweep gas (both having the same value); the pressure difference between the two sides was always maintained at a very low level (~0.1−0.2 in. of water). Measurements were made for water vapor and N_2 permeation rates to check whether higher gas flow rates affected N_2 permeation rates since boundary layer resistances were not expected to affect the very low N_2 permeability (N_2 has a very high partial pressure difference compared to that for water). Figure 9 provides the data.

The left-hand side inset in Figure 9 illustrates the N_2 data; its transmission rate does not vary much over the gas flow rate range 20−500 cm^3/min. If we convert N_2 permeability data in Table 1 or Figure S7 for the 4 mg membrane, we get a N_2 transmission rate of 735 g/(m^2·day). While this value is somewhat higher than that in Figure 9, the membrane here is

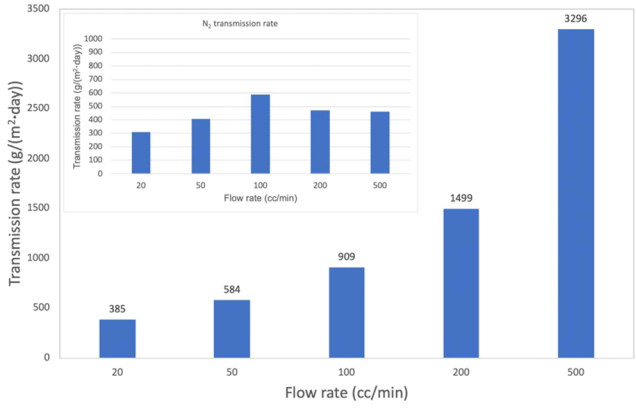

Figure 9. Transmission rates of moisture and N_2 in the DMPC for one 8 mg PES-EDA-GO-PU membrane at 25 °C.

https://dx.doi.org/10.1021/acsami.0c00615
ACS Appl. Mater. Interfaces 2020, 12, 11094−11103

thicker (based on 8 mg GO), cross-linked, and has a PU coating. This clearly shows that the boundary layer resistance has almost no effect on N_2 permeation rates. Further, very little excess pressure difference was created due to higher gas flow rates (see Table S4). On the other hand, the water vapor transmission rate increases substantially going up to 3296 g/(m^2·day) as the gas flow rate increases. This demonstrates that the results from the upright cup method presented earlier will strongly underestimate moisture vapor permeability due to the substantial boundary layer resistance. Without any membrane, the upright cup method yields 1000 g/(m^2·day) for water. The separation factors $\alpha_{H_2O-N_2}$ of H_2O over N_2 for different gas flow rates increase from 105 at the lowest gas flow rate to 439 at the highest gas flow rate.

Literature data provide a commonly cited minimum (threshold) water vapor flux of 2000 g/(m^2·day) that defines a breathable fabric.[32−35] Ref 18 has also cited this value; ref 19 has cited a few others, such as Gore-Tex Pro Shell, which has a somewhat higher value [2800 g/(m^2·day)] than this threshold, whereas SympaTex has a somewhat lower value [1300 g/(m^2·day)] (all at 30 °C). Our value obtained at 25 °C and at the highest gas flow rate is quite above this threshold.

The water vapor flux results from GO-based membranes of ref 18 were for saturated water vapor at 60 °C. Due to the temperature dependence of vapor pressure, they[18] had estimated that their reported values can be a factor of ∼3 higher than fluxes measured at 37 °C. Lowering the temperature to 25 °C will still further reduce their value. Our measured value of 3296 g/(m^2·day) at a 500 cc/min gas flow rate had a ΔRH of ∼82%. If we calculate the water vapor transmission rate corresponding to a ΔRH of 50%, our transmission rate at 25 °C would be reduced to 2064 g/(m^2·day) (Table S4). If we account for enhanced water vapor pressure at 30 °C, the water vapor transmission rate will be enhanced by a factor of 1.35. It is clear that the water transmission rates of GO membranes of this study exceed the minimum threshold value. The carbon nanotube (CNT)-based membrane barrier with sub-5 nm pores is highly water vapor permeable and has a few times higher water vapor flux at 30 °C[19] than the threshold value.

For the separation factors of $\alpha_{H_2O-N_2}$ of H_2O over N_2 for different gas flow rates reported in Figure 9, the transport of each species was measured in separate experiments. The data from Petukhov et al.[16] are also based on the pure component permeability ratio (i.e., "ideal separation factor"); depending on the GO membrane type, it was very high between 95 and 13 260. Moisture permeances through these membranes prepared by spin coating on porous anodic aluminum oxide substrates and pressure-assisted filtration were strongly dependent on the transmembrane pressure, diminishing by an order of magnitude from equipressure conditions to a 0.1 MPa pressure difference.

We explore now the variations in the interlayer gap for the compressed and cross-linked membranes on a PEEK substrate. Figure 10 illustrates the XRD scan results for such a membrane without any PU coating. There are several peaks identifiable for the GO membrane. The diffraction peak at 2θ = 22.80° with a high intensity corresponds to its interlayer spacing (d_{002}) of 0.389 nm.

This decrease in the interlayer spacing between the graphene oxide sheets is attributed to the physical compression; this value is close to an earlier calculated estimate of 0.4 nm

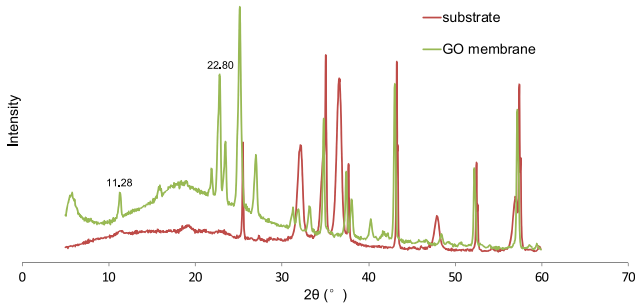

Figure 10. XRD of an 8 mg GO membrane compressed and cross-linked on a porous PEEK substrate without any PU coating.

mentioned just before Figure 2. A 001 peak appears at 2θ = 11.28°. The interlayer distance calculated for this peak is 0.788 nm, which is in agreement with its high degree of oxidation. Another peak is at 15.80°, corresponding to an interlayer spacing of 0.563 nm. The peaks corresponding to various estimates in the interlayer spacing of this GO result from the high degree of disorder and are proportional to the content of oxygen.

In Figure 10, there are two additional smaller sharp peaks on both sides of the peak at ∼22°. These along with other peaks essentially show a distribution of interlayer spacing including some smaller than that at ∼22°. Compression and cross-linking improve the situation; however, the rate and manner of decompression is another variable that allows a bit of spring back.

Permeation tests of CEES through the PEEK-EDA-GO-PU barrier membrane were also carried out in the manner described in Section 2.8.[36] The results are shown in Figure 11. It appears that CEES is completely blocked for 16.2 min by the GO barrier membrane. What is of much greater interest is that after the breakthrough, the GO-based barrier allows in the effluent a very low level of CEES for a long time coming out at almost a constant rate. It shows that the PEEK-EDA-GO-PU membrane has significant potential for blocking CEES under appropriate conditions. We are exploring such aspects.

It is useful to develop an estimate of the effective diffusion coefficient for CEES through this membrane barrier using time lag information. Since time lag, t_{lag}, is related to the effective diffusion coefficient D_o and the membrane thickness by $t_{lag} = (l^2/6D_o)$, where l is the membrane thickness, we can calculate the effective diffusion coefficient of CEES in this structure given t_{lag} to be 16.2 min. The value of D_o turns out to be 6.38 × 10^{-11} cm^2/s; this value is quite low compared to that through butyl rubber (D_o = 2.64 × 10^{-9} cm^2/s).[37] Young's modulus was also determined for a cross-linked and a PU-coated membrane; details and the values are provided in Section S.4 and Figure S9.

4. CONCLUSIONS

A novel GO-based composite membrane structure has been developed. It has either a porous PES or a porous PEEK membrane as the substrate with a GO layer on top developed by vacuum filtration of a GO suspension. After a few modifications such as EDA cross-linking, this membrane has a reasonable water vapor transmission rate, which exceeds the common breathability threshold while it can completely block DMMP for 15 days as shown by the upright cup method. With EDA as a cross-linking agent and polyurethane coating as an

https://dx.doi.org/10.1021/acsami.0c00615
ACS Appl. Mater. Interfaces 2020, 12, 11094−11103

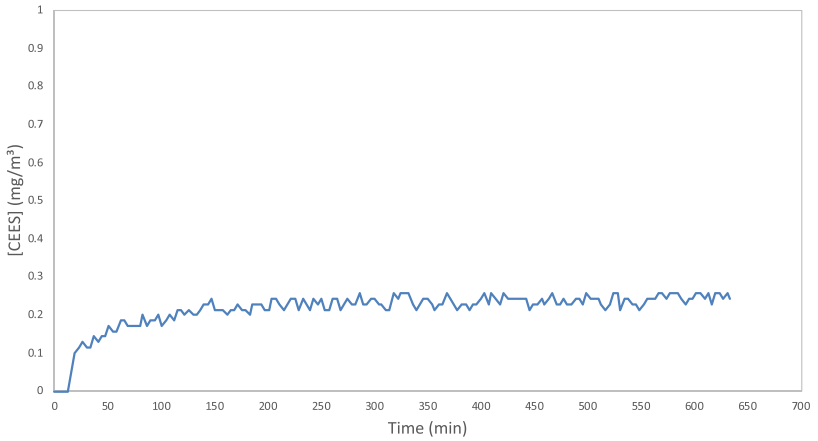

Figure 11. Permeation results for CEES for the PEEK-EDA-GO-PU membrane.

antiscratching layer, the mechanical property of this membrane has been greatly improved in that the membrane can be bent without damage to species permeances, the selectivity of water vis-à-vis other gas/vapor species, as well as blocking of DMMP. Permeation behaviors of several gases/vapors, e.g., He, N_2, and ethane, have been studied using the dynamic moisture permeation cell (DMPC). For the PEEK-EDA-GO-PU membranes after bending, the separation factors of H_2O over various species for low gas flow rates in the DMPC are as follows: α_{H_2O-He} is 42.35, $\alpha_{H_2O-N_2}$ is 110.77, and $\alpha_{H_2O-ethane}$ is 1800. At higher gas flow rates in the DMPC, the boundary layer resistances to water vapor transmission due to high-moisture permeability are reduced substantially and the moisture transmission rate is considerably enhanced. Under high gas flow rates, the water vapor to nitrogen selectivity went up to 439. Permeation tests of CEES were also carried out. The PEEK-EDA-GO-PU membrane can completely block CEES for some time and then allows an extremely low rate of steady CEES permeation.

■ ASSOCIATED CONTENT

Supporting Information

The Supporting Information is available free of charge at https://pubs.acs.org/doi/10.1021/acsami.0c00615.

Parameters of PES and PEEK support membranes; graphical summary of steps in membrane fabrication; gas permeation measurement details; dynamic moisture permeation cell for gas permeation; upright cup method and the cell used; photos of GO membranes for varying GO levels in suspension; SEM images of GO membrane cross-section with different thicknesses; laminate gap calculations; schematic picture of the graphene layer; permeance of various species and the membrane thickness; cup method results for water vapor and toluene; cup method results for water vapor and DMMP; cross-linked GO membrane made on a PEEK support membrane; moisture transmission rate calculation for DMPC; Young's modulus of various PES substrate-based membranes (PDF)

■ AUTHOR INFORMATION

Corresponding Author

Kamalesh K. Sirkar − *Department of Chemical and Materials Engineering, New Jersey Institute of Technology, Newark, New Jersey 07102, United States;* orcid.org/0000-0001-7157-5010; Phone: 973-596-8447; Email: sirkar@njit.edu; Fax: 973-642-4854

Authors

Cheng Peng − *Materials Science and Engineering, New Jersey Institute of Technology, Newark, New Jersey 07102, United States*

Zafar Iqbal − *Department of Chemistry and Environmental Science, New Jersey Institute of Technology, Newark, New Jersey 07102, United States*

Gregory W. Peterson − *U.S. Army Combat Capabilities Development Command Chemical Biological Center, FCDD-CBR-PF, Aberdeen Proving Ground, Maryland 21010-5424, United States;* orcid.org/0000-0003-3467-5295

Complete contact information is available at: https://pubs.acs.org/10.1021/acsami.0c00615

Notes

The authors declare no competing financial interest.

■ ACKNOWLEDGMENTS

The authors gratefully acknowledge support for this research from DTRA contract # HDTRA 1-16-1-0028. This research was carried out in the NSF Industry/University Cooperative Research Center for Membrane Science, Engineering and Technology that has been supported via two NSF Awards IIP1034710 and IIP-1822130. The authors thank Matt Browe for conducting the CEES permeation tests.

■ REFERENCES

(1) Nagarajan, R.; Zukas, W.; Hatton, T. A.; Lee, S. *Nanoscience and Nanotechnology for Chemical and Biological Defense*; ACS Symposium Series; American Chemical Society, 2009; Vol. *1016*.

(2) Romano, J. A., Jr.; Salem, H.; Lukey, B. J.; Lukey, B. J. *Chemical Warfare Agents: Chemistry, Pharmacology, Toxicology, and Therapeutics*; CRC Press, 2007; pp 21−50.

(3) Napadensky, E.; Elabd, Y. A. *Breathability and Selectivity of Selected Materials for Protective Clothing*, No. ARL-TR-3235; Army Research Lab Aberdeen Proving Ground MD Weapons and Materials Research Directorate, 2004.

(4) Glover, T. G.; Peterson, G. W.; Schindler, B. J.; Britt, D.; Yaghi, O. MOF-74 building unit has a direct impact on toxic gas adsorption. *Chem. Eng. Sci.* **2011**, *66*, 163−170.

(5) Nair, R. R.; Wu, H. A.; Jayaram, P. N.; Grigorieva, I. V.; Geim, A. K. Unimpeded permeation of water through helium-leak–tight graphene-based membranes. *Science* **2012**, *335*, 442–444.
(6) Hummers, W. S., Jr.; Offeman, R. E. Preparation of graphitic oxide. *J. Am. Chem. Soc.* **1958**, *80*, 1339.
(7) Dikin, D. A.; Stankovich, S.; Zimney, E. J.; Piner, R. D.; Dommett, G. H.; Evmenenko, G.; Nguyen, S. T.; Ruoff, R. S. Preparation and characterization of graphene oxide paper. *Nature* **2007**, *448*, 457–460.
(8) Eda, G.; Chhowalla, M. Chemically derived graphene oxide: towards large-area thin-film electronics and optoelectronics. *Adv. Mater.* **2010**, *22*, 2392–2415.
(9) Yoo, B. M.; Shin, J. E.; Lee, H. D.; Park, H. B. Graphene and graphene oxide membranes for gas separation applications. *Curr. Opin. Chem. Eng.* **2017**, *16*, 39–47.
(10) Aher, A.; Cai, Y.; Majumder, M.; Bhattacharyya, D. Synthesis of graphene oxide membranes and their behavior in water and isopropanol. *Carbon* **2017**, *116*, 145–153.
(11) Lee, J.; Chae, H. R.; Won, Y. J.; Lee, K.; Lee, C. H.; Lee, H. H.; Kim, I. C.; Lee, J. M. Graphene oxide nanoplatelets composite membrane with hydrophilic and antifouling properties for wastewater treatment. *J. Membr. Sci.* **2013**, *448*, 223–230.
(12) Huang, K.; Liu, G.; Lou, Y.; Dong, Z.; Shen, J.; Jin, W. A graphene oxide membrane with highly selective molecular separation of aqueous organic solution. *Angew. Chem.* **2014**, *126*, 7049–7052.
(13) Kim, H. W.; Yoon, H. W.; Yoon, S. M.; Yoo, B. M.; Ahn, B. K.; Cho, Y. H.; Shin, H. J.; Yang, H.; Paik, U.; Kwon, S.; Choi, J. Y. Selective gas transport through few-layered graphene and graphene oxide membranes. *Science* **2013**, *342*, 91–95.
(14) Liu, R.; Gong, T.; Zhang, K.; Lee, C. Graphene oxide papers with high water adsorption capacity for air dehumidification. *Sci. Rep.* **2017**, *7*, No. 9761.
(15) Eliseev, A. A.; Poyarkov, A. A.; Chernova, E. A.; Eliseev, A. A.; Chumakov, A. P.; Konovalov, O. V.; Petukhov, D. I. Operando study of water vapor transport through ultra-thin graphene oxide membranes. *2D Mater.* **2019**, *6*, No. 035039.
(16) Petukhov, D. I.; Chernovaa, E. A.; Kapitanovab, O. O.; Boytsovaa, O. V.; Valeev, R. G.; Chumakove, A. P.; Konovalove, O. V.; Eliseev, A. A. Thin graphene oxide membranes for gas dehumidification. *J. Membr. Sci.* **2019**, *577*, 184–194.
(17) Chen, P.-Y.; Zhang, M.; Liu, M.; Wong, I. Y.; Hurt, R. H. Ultrastretchable Graphene-Based MolecularBarriers for Chemical Protection, Detection, and Actuation. *ACS Nano* **2018**, *12*, 234–244.
(18) Spitz Steinberg, R.; Cruz, M.; Mahfouz, N. G. A.; Qiu, Y.; Hurt, R. H. Breathable Vapor Toxicant Barriers Based on Multilayer Graphene Oxide. *ACS Nano* **2017**, *11*, 5670–5679.
(19) Bui, N.; Meshot, E. R.; Kim, S.; Peña, J.; Gibson, P. W.; Wu, K. J.; Fornasiero, F. Ultrabreathable and Protective Membranes with Sub-5 nm Carbon Nanotube Pores. *Adv Mater.* **2016**, *28*, 5871–5877.
(20) Li, H.; Song, Z.; Zhang, X.; Huang, Y.; Li, S.; Mao, Y.; Ploehn, H. J.; Bao, Y.; Yu, M. Ultrathin, molecular-sieving graphene oxide membranes for selective hydrogen separation. *Science* **2013**, *342*, 95–98.
(21) Shivaraman, S.; Chandrashekhar, M. V. S.; Boeckl, J. J.; Spencer, M. G. Thickness estimation of epitaxial graphene on SiC using attenuation of substrate Raman intensity. *J. Electron. Mater.* **2009**, *38*, 725–730.
(22) Lin, L. Y.; Kim, D. E.; Kim, W. K.; Jun, S. C. Friction and wear characteristics of multi-layer graphene films investigated by atomic force microscopy. *Surf. Coat. Technol.* **2011**, *205*, 4864–4869.
(23) Jung, I.; Vaupel, M.; Pelton, M.; Piner, R.; Dikin, D. A.; Stankovich, S.; An, J.; Ruoff, R. S. Characterization of thermally reduced graphene oxide by imaging ellipsometry. *J. Phys. Chem. C* **2008**, *112*, 8499–8506.
(24) Kuila, T.; Mishra, A. K.; Khanra, P.; Kim, N. H.; Uddin, M. E.; Lee, J. H. Facile method for the preparation of water dispersible graphene using sulfonated poly (ether–ether–ketone) and its application as energy storage materials. *Langmuir* **2012**, *28*, 9825–9833.
(25) Hung, W. S.; Tsou, C. H.; De Guzman, M.; An, Q. F.; Liu, Y. L.; Zhang, Y. M.; Hu, C. C.; Lee, K. R.; Lai, J. Y. Cross-linking with diamine monomers to prepare composite graphene oxide-framework membranes with varying d-spacing. *Chem. Mater.* **2014**, *26*, 2983–2990.
(26) Gibson, P. W.; Kendrick, C. E.; Rivin, D.; Charmchi, M. An Automated Dynamic Water Vapor Permeation Test Method. *Performance of Protective Clothing*; ASTM International, 1997; Vol. *6*.
(27) Lide, D. R. *CRC Handbook of Chemistry and Physics: A Ready-Reference Book of Chemical and Physical Data*; CRC Press, 1995.
(28) Relative humidity to absolute humidity and vice versa calculators. https://planetcalc.com/2167/ (accessed Aug 23, 2017).
(29) LaFrate, A. L.; Gin, D. L.; Noble, R. D. High water vapor flux membranes based on novel diol– imidazolium polymers. *Ind. Eng. Chem. Res.* **2010**, *49*, 11914–11919.
(30) McCullough, E. A.; Kwon, M.; Shim, H. A comparison of standard methods for measuring water vapour permeability of fabrics. *Meas. Sci. Technol.* **2003**, *14*, 1402–1408.
(31) Kanan, S. M.; Waghe, A.; Jensen, B. L.; Tripp, C. P. Dual WO_3 based sensors to selectively detect DMMP in the presence of alcohols. *Talanta* **2007**, *72*, 401–407.
(32) Wartell, M. A.; Kleinman, M. T.; Huey, B. M.; Duffy, L. M. *Strategies to Protect the Health of Deployed U.S. Forces: Force Protection and Decontamination*; The National Academies Press: Washington, DC, 1999.
(33) Lomax, G. R. Breathable Polyurethane Membranes for Textile and Related Industries. *J. Mater. Chem.* **2007**, *17*, 2775–2784.
(34) Rother, M.; Barmettler, J.; Reichmuth, A.; Araujo, J. V.; Rytka, C.; Glaied, O.; Pieles, U.; Bruns, N. Self-Sealing and Puncture Resistant Breathable Membranes for Water-Evaporation Applications. *Adv. Mater.* **2015**, *27*, 6620–6624.
(35) Gugliuzza, A.; Drioli, E. A Review on Membrane Engineering for Innovation in Wearable Fabrics and Protective Textiles. *J. Membr. Sci.* **2013**, *446*, 350–375.
(36) Peterson, G. W.; DeCoste, J. B.; Fatollahi-Fard, F.; Britt, D. K. Engineering UiO-66-NH_2 for toxic gas removal. *Ind. Eng. Chem. Res.* **2014**, *53*, 701–707.
(37) Dubey, V.; Maiti, S. N.; Rao, N. B.; Gupta, A. K. Study of permeation of bis (2-chloroethyl) sulfide through elastomer membranes. *Polym.-Plast. Technol. Eng.* **1997**, *36*, 445–460.

https://dx.doi.org/10.1021/acsami.0c00615
ACS Appl. Mater. Interfaces 2020, 12, 11094–11103